Trends in Genetics

CellPress

Feature Review

DNA Repair Pathway Choices in CRISPR-Cas9-Mediated Genome Editing

Chaoyou Xue[1,2] and Eric C. Greene[1,*]

Many clustered regularly interspaced short palindromic repeats (CRISPR)-CRISPR-associated protein 9 (Cas9)-based genome editing technologies take advantage of Cas nucleases to induce DNA double-strand breaks (DSBs) at desired locations within a genome. Further processing of the DSBs by the cellular DSB repair machinery is then necessary to introduce desired mutations, sequence insertions, or gene deletions. Thus, the accuracy and efficiency of genome editing are influenced by the cellular DSB repair pathways. DSBs are themselves highly genotoxic lesions and as such cells have evolved multiple mechanisms for their repair. These repair pathways include homologous recombination (HR), classical nonhomologous end joining (cNHEJ), microhomology-mediated end joining (MMEJ) and single-strand annealing (SSA). In this review, we briefly highlight CRISPR-Cas9 and then describe the mechanisms of DSB repair. Finally, we summarize recent findings of factors that can influence the choice of DNA repair pathway in response to Cas9-induced DSBs.

Highlights

Clustered regularly interspaced short palindromic repeats (CRISPR)-CRISPR-associated protein 9 (Cas9)-mediated genome editing offers a powerful approach as a potential therapy for monogenic human genetic diseases.

Precise template-free base deletions can be achieved through microhomology-mediated end joining (MMEJ) repair and depend on local target site sequence.

The DNA repair pathway choice in CRISPR-Cas9 induced-double-strand breaks (DSBs) is regulated by several key factors including the cell cycle, target site sequence and chromatin structure, and the identity of the donor DNA template.

Homology-directed repair (HDR)-related DNA repair pathways in response to CRISPR-Cas9 induced-DSBs in mammalian cells are complicated and relatively inefficient. Different DNA repair pathways might be used to repair each end at a DSB resulting in the potential for asymmetric repair.

Introduction

DSB repair mechanisms have been harnessed for genome editing, based on the use of engineered nucleases that introduce DSBs at target sites, and relies on these DNA repair pathways to insert, delete, or replace pieces of DNA [1]. Examples of engineered nucleases include zinc-finger nucleases (**ZFNs**; see Glossary) [2], transcription activator-like effector nucleases (**TALENS**) [3], and the **CRISPR**-Cas-based RNA guided DNA endonucleases [4–8]. DSBs genotoxic DNA lesions, which if left unrepaired can cause chromosomal rearrangements, genomic instability, and cell death. Eukaryotes have numerous pathways to repair DSBs [9–12]. Two major pathways include error-free, template-dependent HR, and the error-prone, template-independent cNHEJ [9,10]. Additional pathways include MMEJ and SSA, both of which are more error-prone [11,12].

Genome editing is achieved through homology-directed repair (**HDR**) of the resulting DSB, however, mammalian cells often prefer to repair DSBs by error-prone repair pathways, such as cNHEJ, which can generate undesirable mutations. The term HDR does not represent a single DNA repair pathway. Instead, HDR is related to the nature of DNA donor templates used to guide the DNA repair reaction, including double-stranded DNA donor templated repair (**DSTR**) and single-stranded DNA donor templated repair (**SSTR**) [13].

Here, we briefly describe the CRISPR-Cas9 system. We then discuss the different DSB repair pathways, focusing mainly on mammalian DSB repair mechanisms. Finally, we discuss how CRISPR-Cas9-induced DSBs are repaired by the host cell and the factors that influence the choice of repair pathway.

[1]Department of Biochemistry and Molecular Biophysics, Columbia University, New York, NY 10032, USA
[2]Present address: Tianjin Institute of Industrial Biotechnology, Chinese Academy of Sciences, Tianjin, China

*Correspondence:
ecg2108@cumc.columbia.edu (E.C. Greene).

Overview of the Cas9 CRISPR-Cas System

CRISPR technologies have emerged as powerful tools for genome engineering [5–7]. The fundamental basis for genome editing using the CRISPR protein **Cas9** is the ability to introduce a precise DSB within a genome based upon sequence complementarity with the guide (g)RNA (Box 1) [1].

Cas9 Nuclease Activity

Cas9 is a large multidomain protein comprising a recognition lobe, which is formed of the REC1, REC2, and REC3 domains, and a nuclease lobe, which is composed of a protospacer-adjacent motif (**PAM**)-interacting domain and two nuclease domains: a RuvC-like domain and an HNH-like domain (Figure 1A) [4,8,14]. PAM recognition triggers initial unwinding of the adjacent double-strand (ds)DNA (referred to as the seed region), allowing the gRNA to begin forming an RNA–DNA hybrid (Figure 1A) [15,16]. If the DNA sequence is fully complementary to the gRNA, then there can be further RNA–DNA hybrid formation, resulting in the formation of a stable **R-loop** [16]. During R-loop formation, the Cas9 protein undergoes a conformational change to activate its nuclease activity [17,18], allowing the HNH-like domain to cut the target DNA strand three base pairs upstream from the PAM, while the RuvC-like nuclease domain cuts 3–5 bps away on the non-target strand (Figure 1A) [19].

Off-target effects arise from the ability of Cas9 to tolerate mismatches between the gRNA and potential dsDNA targets [20–22]. A single base mismatch in the PAM or seed region can reduce Cas9 cleavage activity, but mismatches within the PAM-distal region are tolerated [4]. To address this problem, high-fidelity variants of Cas9 have been developed [17,18,23–26]. For example, eSpCas9(1.1) decreases off-target effects by weaking interactions between the protein and the non-targeted DNA strand, such that partial DNA–RNA pairing interactions are less tolerated [23]. SpCas9-HF1 decreases off-target effects by reducing interactions between the protein and the targeted DNA strand [24], whereas HypaCas9 prevents DNA cleavage when there are mismatches between the gRNA and potential off-target sites [17,18]. Cas9 mutations in the REC3 domain, which affect the activation of Cas9 after DNA binding, also enhance target recognition fidelity [25,26]. Development of these higher-fidelity Cas9 variants could be beneficial for clinical applications.

Box 1. Overview of CRIPSR-Cas Systems

The first CRISPR locus was discovered more than three decades ago [189–191]. However, the function of these loci was not recognized until 20 years later [192]. In 2007, Barrangou *et al.* demonstrated that CRISPR loci represent an adaptive immune system, which can 'memorize' past viral infections by inserting viral genetic fragments into the host CRISPR array [192]. The CRISPR array is transcribed and processed into mature CRISPR RNAs (crRNAs, also referred to as guide RNA or gRNA), which assemble with Cas effector proteins [193]. Using the crRNAs as guides, viral genomes are targeted through sequence-specific DNA-RNA base pairing interactions and then destroyed [192,194–196]. CRISPR-Cas systems can be divided into two classes (Class 1 and Class 2), each of which contains three types [197]. Class 1 systems are further subdivided into types I, III, and IV, whereas Class 2 systems are subdivided into types II, V, and VI [197]. Importantly, Class 2 CRISPR-Cas systems, such as Cas9, require just one protein component for interference, thus offering a significant advantage as genome editing tools [197]. Cas9 is the effector protein of type II CRISPR-Cas systems and is the first CRISPR-associated effector protein that was repurposed for genome editing (see Figure 1A in main text) [1]. In nature, Cas9 requires two RNA molecules, a crRNA and a *trans*-activating crRNA (tracrRNA), which base pairs with the repeat sequence of the crRNA [4,8,198]. The resulting Cas9-RNA complex must recognize a short DNA sequence motif called the protospacer-adjacent motif (PAM) and then test the flanking dsDNA for sequence complementarity to the crRNA (Figure 1A) [15]. For genome engineering, the crRNA and tracrRNA can be combined into a single guide-RNA (sgRNA) without affecting Cas9-mediated target binding and cleavage activities; we use the general term 'gRNA' to represent either the single sgRNA or dual tracrRNA-crRNA (Figure 1A) [4–7]. The Cas9-gRNA complex must recognize a short DNA sequence motif called the PAM and then test the flanking dsDNA for sequence complementarity to the crRNA (Figure 1A) [15]. When Cas9 binds to the correct dsDNA target it cleaves the DNA to yield either blunt or staggered ends (Figure 1A) [14,19]. Genome editing is achieved during the repair of the resulting DSB [199]. Notably, Cas9 can potentially recognize and cleave DNA sites that may not perfectly match the sgRNA or tracrRNA-crRNA, which has the potential to cause off-target genome mutations [20–22,199,200].

Glossary

BLM: Bloom helicase is a member of the RECQ helicase family. BLM mutations are associated with the disease Bloom's syndrome, which is characterized by a greatly increased cancer risk.
BRCA1-BARD1: breast cancer type 1 susceptibility protein (BRCA1) and BRCA1-associated RING domain 1 (BARD1) form a heterodimeric protein complex that plays essential roles in maintaining genome integrity.
Cas9: CRISPR-associated protein 9 is an RNA-guided endonuclease from the CRISPR adaptive immune system from *Streptococcus pyogenes*. Cas9 has emerged as a prominent tool in the genome engineering field.
CRISPR: clustered regularly interspaced short palindromic repeats are bacterial chromosomal loci consisting of short DNA sequences derived from the genomes of foreign pathogens. CRISPR loci provide a 'memory' of past infections, allowing Cas proteins to detect and destroy any similar foreign pathogens during subsequent infections.
DSTR: double-stranded DNA donor templated repair, refers to any HDR mechanism that utilizes a dsDNA as a template to guide DNA repair.
HDR: homology-directed repair refers to any DNA repair mechanism that utilizes a homologous DNA donor to help guide the repair of broken DNA molecules.
PAM: the Protospacer adjacent motif or PAM is a short DNA sequence required by Cas9 to recognize a potential DNA cleavage site. PAMs are found in invading DNA but are not present in the bacterial CRISPR locus, enabling Cas9 to identify and destroy pathogenic viruses or plasmids without harming the bacterial chromosome.
R-loop: refers to a double-stranded nucleic acid structure comprised of one DNA strand and one RNA strand.
RAD51: a protein that forms long helical filaments on ssDNA. RAD51 filaments pair the ssDNA with a related (i.e., homologous) dsDNA found elsewhere in the genome. This pairing step allows repair to take place using the homologous DNA as a template to copy any missing genetic information.
RAD51 paralogs: proteins that are closely related to RAD51; promote HR by stimulating the assembly and/or stability of RAD51 filaments. Mammals

Guide RNAs

The gRNA can be produced either *in situ* or *ex situ* [27]. For instance, the gRNA can be produced intracellularly via transcription from a plasmid template or from a viral DNA [e.g., adeno-associated viruses (AAV), adenovirus (AdV), and lentivirus (LV)] and the resulting gRNA will bind to co-expressed Cas9 protein to form the active Cas9-gRNA complex (Figure 1B) [28–31]. The gRNA can also be produced using *in vitro* transcription or chemical synthesis (Figure 1B) [32]. An advantage of *ex situ* gRNA production is that the gRNAs can be synthesized with chemical modifications that can protect the gRNA from digestion by cellular nucleases [33,34]. Chemical gRNA modifications can also alter the thermodynamic stability of the gRNA-target dsDNA to improve target recognition and decrease off-target activity [33,34]. gRNAs produced by chemical synthesis can also include chemical modifications to reduce cellular toxicity and inhibit type I interferon α (IFN-α) related proinflammatory cytokine response, which is induced by single-strand (ss)RNA recognition through the Toll-like receptor 7 (TLR7) (Figure 1B) [35,36].

Cas9-gRNA Delivery

Genome editing requires delivery of Cas9-gRNA to the cell nucleus (Figure 1B). Timing and dosage are important factors that can be modulated to prevent undesirable off-target effects [37,38]. Currently, there are three major delivery methods (Figure 1B). First, the mature Cas9-gRNA ribonucleoprotein (RNP) can be delivered using gold nanoparticles or lipid nanoparticles [38–40]. This delivery method provides control over the timing and dosage of the Cas9-gRNA. However, delivering such a large RNP can be challenging and its introduction has the potential to trigger immunological responses [41]. Second, genes encoding Cas9 and the gRNA can be delivered with a DNA vector (Figure 1B) [6,7,30,42]. Although, this method allows for long-term Cas9 and gRNA expression, however, persistent expression of the Cas9 complex might increase potential for off-target effects [32,43,44]. In addition, cellular receptors that sense exogenous DNA, including the Toll-like receptor 9 (TLR9), melanoma 2 (AIM2), and cyclic GMP-AMP synthase-stimulator of interferon genes (cGAS-STING), can cause cytotoxic effects and induce IFN-α related immune responses (Figure 1B) [45–48]. Third, the gRNA can be delivered along with an mRNA encoding Cas9 [33]. This approach allows for transient Cas9 expression, which can help mitigate off-target events [27], but may have limited efficiency due to rapid degradation of the Cas9-encoding mRNA [33]. Several strategies have been developed to allow for conditional activation of Cas9 *in situ*, and for a more detailed discussion of these methods we refer readers to several recent reviews [27,49–51].

Cas9 is currently being evaluated in several early clinical trials, including studies targeting genetic diseases such as sickle cell anemia and β-thalassemia (Phase I/II; ClinicalTrials.gov ID: NCT03745287 and NCT03655678), cancers such as B cell and non-Hodgkin lymphomas (Phase I; ClinicalTrials.gov ID: NCT04035434), multiple myeloma (Phase I; ClinicalTrials.gov ID: NCT04244656), and leukemia and lymphoma (Phase I/II, Clinicaltrials.gov ID: NCT03166878) [52]. In addition to Cas9, the type V CRISPR-Cas12a (formerly named Cpf1) system has received widespread attention due to several advantages [53]. First, Cas12a is smaller than Cas9 and easier to deliver in clinical applications [53]. Second, Cas12a is guided by a single CRISPR (cr)RNA that is less than half the size of the short guide (sg)RNA for Cas9 [54]. In addition, the CRISPR-Cas12a system is considered to have lower off-target efficiency, which may be related to its lower nuclease activities [55,56]. Moreover, Cas12a cleaves dsDNA with 4–5 bp staggered 5′ overhangs, in contrast to the mixed blunt and 1–2 bp staggered 5′ overhangs of Cas9, which might affect DNA repair outcomes (see later) [54]. However, the recently discovered Cas12a cis (target-dependent) and trans dsDNA (target-independent) nicking and cleavage activities may be detrimental for genome editing and need careful evaluation [57,58].

have two primary RAD51 paralog complexes called CX3, comprised of RAD51C and XRCC3, and BCDX2, comprised of RAD51B, RAD51C, RAD51D, and XRCC2.

RPA: replication protein A is a ssDNA binding protein that protects ssDNA from nucleases and prevents formation of secondary structures. RPA is involved in many reactions that include an ssDNA intermediate.

SSTR: single-stranded DNA donor templated repair, refers to any HDR mechanism that utilizes a single-stranded DNA as a template to guide DNA repair.

TALENS: transcription activator-like effector nucleases are artificial endonucleases made up of short (33–35 amino acid) DNA-binding modules called TALEs and can be engineered to cut any desired DNA sequence.

ZFNs: zinc-finger nucleases are artificial endonucleases that consist of a designed zinc-finger protein (ZFP) fused to the cleavage domain of a restriction enzyme.

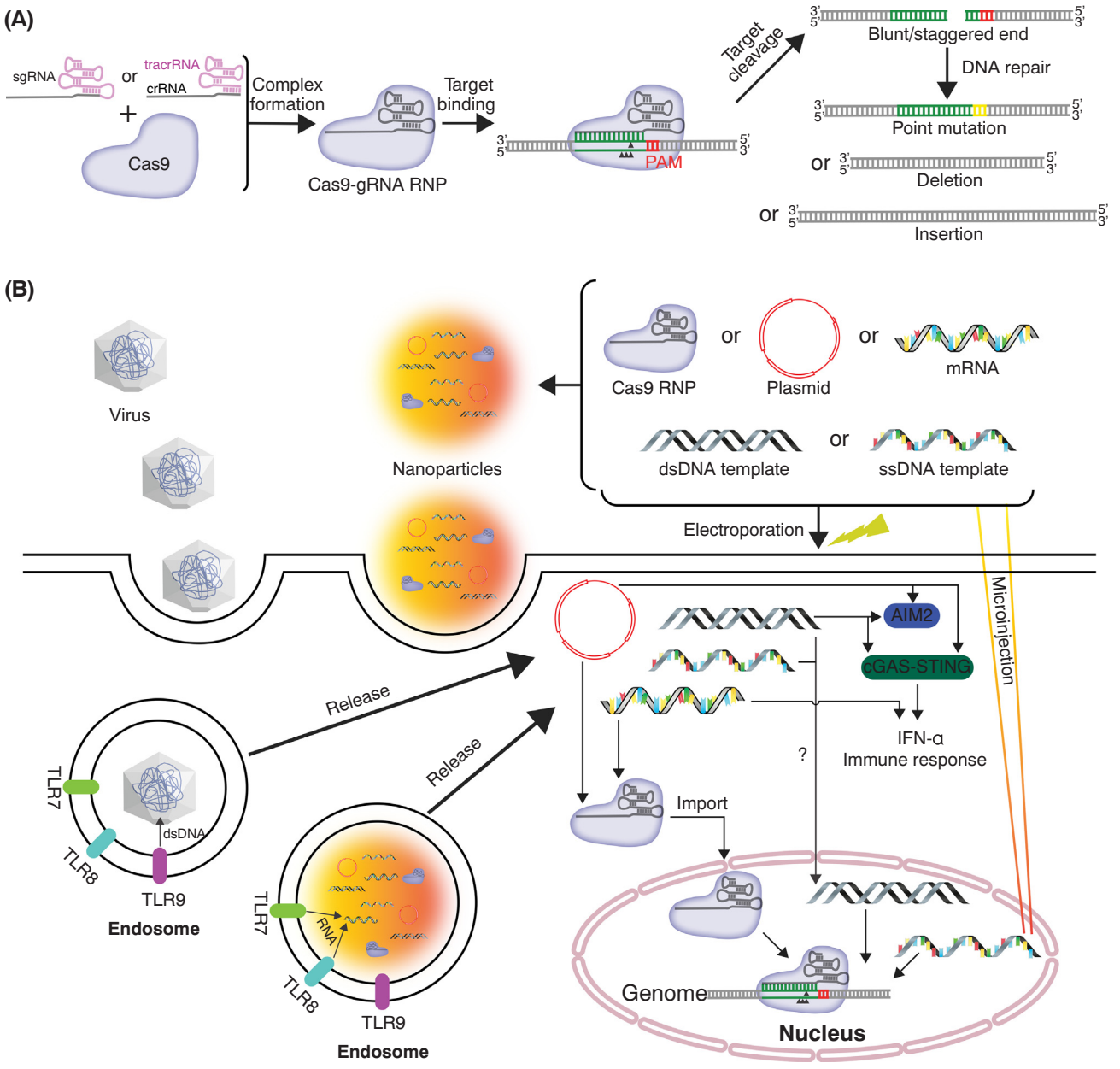

Figure 1. Clustered Regularly Interspaced Short Palindromic Repeats (CRISPR)- CRISPR-Associated Protein 9 (Cas9) Delivery. (A) Mechanism of CRISPR-Cas9 genome editing. A short guide (sg)RNA/*trans*-activating CRISPR (tracr)RNA-CRISPR (cr)RNA associates with the Cas9 endonuclease to form the Cas9-gRNA complex. The gRNA guides Cas9 to its target site of the genomic DNA by recognizing the protospacer-adjacent motif (PAM). When Cas9 binds to the correct double strand (ds)DNA target, its HNH and RuvC nuclease domains cleave the DNA to yield either blunt or staggered ends. Genome editing is achieved during the repair of the resulting double-stranded break (DSB), resulting in precise mutations, gene deletions, or sequence insertions. (B) Cas9 can be delivered in three forms. First, introducing Cas9-gRNA ribonucleoprotein (RNP) complex and DNA templates directly through nanoparticles, electroporation, or microinjection. Second, delivering a plasmid DNA or viral vector for Cas9 and gRNA production *in situ*. Third, delivering separate gRNA together with mRNA for Cas9 protein expression inside the cell. With the exception of microinjection, during which Cas9 components can be directly injected into the nucleus, other delivery methods release Cas9 components into the cytosol. DNA sensing receptors in endosome or cytosol, including the Toll-like receptor 9 (TLR9), melanoma 2 (AIM2) and cyclic GFP-AMP synthase-stimulator of interferon genes (cGAS-STING), drive cell immune responses to foreign DNA. mRNA can also be recognized by TLR7 and TLR8 in endosomes causing mRNA degradation and type I interferon α (IFN-α)-mediated immune responses. Cas9 in the cytosol can be directed into nucleus through nuclear localization sequence; how plasmid DNA, viral DNA and DNA templates enter the nucleus remains unknown.

Double-Strand Break Repair Pathways

In eukaryotic cells, the most prevalent DSB repair pathways include cNHEJ, MMEJ, SSA, and HR (Figure 2). Here, we briefly discuss these different repair pathways and highlight the advantages and disadvantages of each.

Classical Nonhomologous End Joining

cNHEJ is used for re-ligating broken DNA ends, but it is inaccurate and often leads to new mutations [10]. During cNHEJ, DSBs are repaired by directly ligating the broken ends together with minimal DNA end processing (Figure 2A) [10]. cNHEJ is initiated when the ring-shaped Ku70/Ku80 protein heterodimer binds to the DSB ends, which protects the DNA ends from further resection and also recruits the DNA-dependent protein kinase (DNA-PK) [59,60]. DNA-PK recruits the DNA ligase IV–X-ray cross complementing group 4–XRCC4-like factor (LigIV-XRCC4-XLF) complex to ligate the DSB ends [61–63]. When the DSBs ends are not directly ligatable, additional proteins including Artemis nuclease, polynucleotide kinase 3′ phosphatase (PNKP) and DNA polymerases, such as Polμ and Polλ, are required for end processing (Figure 2A) [64–66]. For Cas9-induced DSBs, Cas9 asymmetrically releases the PAM-proximal end of the cleaved DNA within minutes while the PAM-distal end of the DSB remains bound by Cas9 for a longer time period [67,68]. As a result, the PAM-proximal DSB end is exposed for further processing, whereas the other end may be temporally blocked from further processing by the still bound Cas9 [68]. RNA-polymerase and facilitates chromatin transcription (FACT) can remove Cas9 from the PAM-distal side, but how Cas9 is removed during genome editing remains unclear [68,69]. How the tight binding of Cas9 to the PAM-distal DSB end affects DSB repair pathway choice is also unclear.

Given that cNHEJ is an inaccurate repair pathway, several groups are pursuing strategies to inhibit cNHEJ in favor of the much more accurate repair that is achieved through HR. For example, HR-mediated gene editing in mammalian cells can be increased by blocking LigIV activity using small molecules [70–72] or by stimulating proteolytic degradation of LigIV [72]. Suppression of DNA-PK or Ku also promotes DSBs repair through HR [72–75].

Microhomology-Mediated End Joining

MMEJ begins with short-range resection of the DSB (Figure 2B). Like cNHEJ, MMEJ does not require a template for repairing the damaged DNA (Figure 2C) [11]. Instead, the DSB ends are realigned using short (5–25 base pairs) microhomologous sequences present near the broken DNA ends (Figure 2C) [76]. Any remaining 3′ ssDNA flaps are cleaved off, which results in the loss of sequence information [11,76]. The remaining gaps are filled in through DNA synthesis, and the remaining nicks are sealed through ligation [77,78].

During MMEJ, some short-range end resection generates short ssDNA overhangs (~20 bps; Figure 2C) [79]. Short-range end resection promotes MMEJ, whereas more extensive end resection favors SSA and HR (see later; Figure 2D) [80,81]. In mammalian cells, the damage-sensing MRN complex (MRE11-RAD50-NBS1), together with its interacting partner CtIP (C-terminal binding protein interacting protein), initiates end resection (Figure 2C) [82,83]. CtIP phosphorylation during S/G2 phases stimulates the MRE11 endonuclease activity which generates a nick at the 5′ strand near to the DSB end and prevents cNHEJ by removing Ku from the DNA-ends [83–85]. The resulting nick allows the 3′ to 5′ MRE11 exonuclease activity to generate short 3′ overhangs which can be used to initiate MMEJ [79,86]. Inhibition of MMEJ by blocking the ligase activities of DNA ligase (Lig)I and III (involved in the last step of MMEJ; see below) with small molecule inhibitors can promote DSB repair through the more accurate HR pathway [72,87].

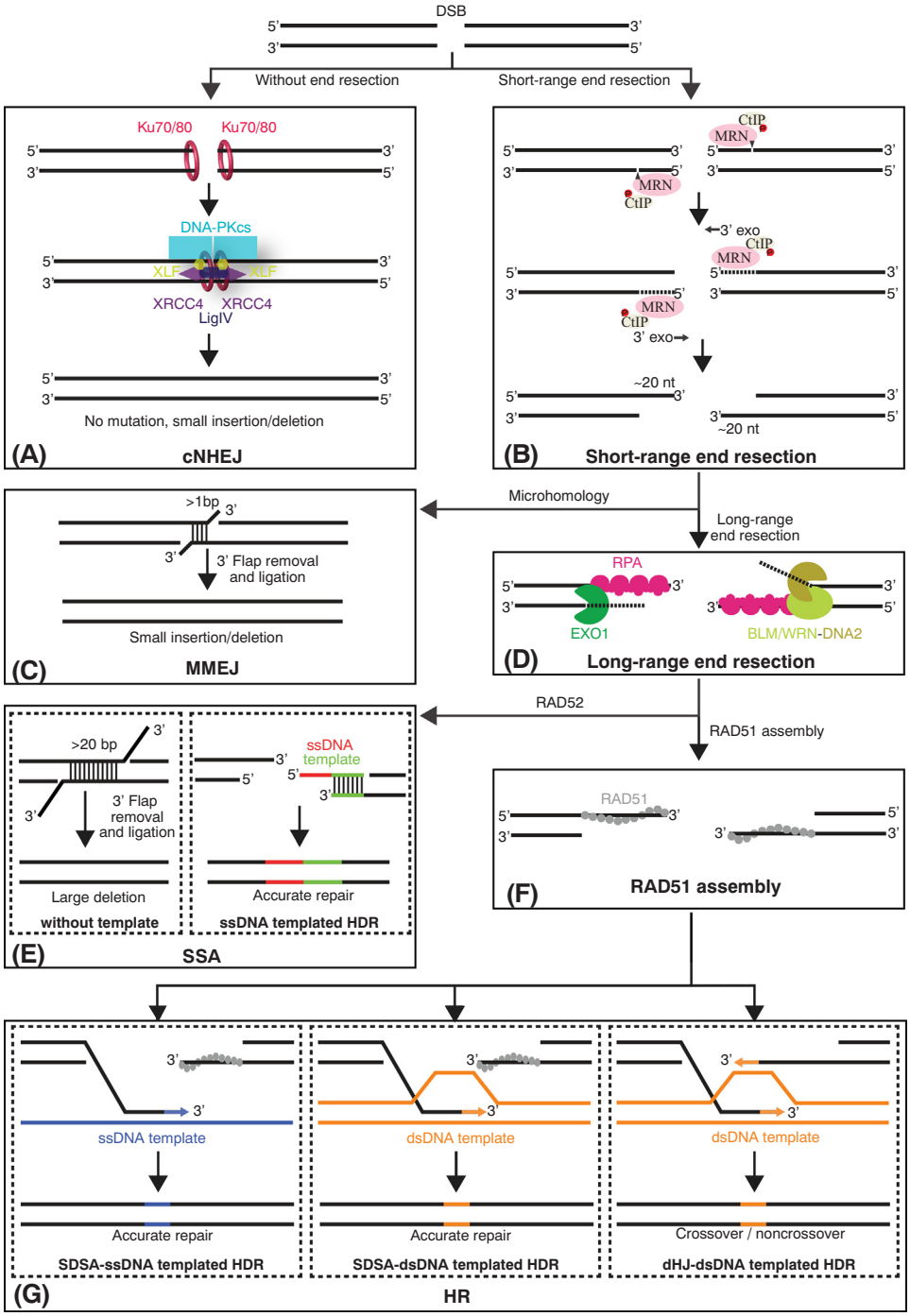

Figure 2. The Four Major Pathways to Repair DNA Double-Strand Breaks (DSBs). (A) Unprocessed DSBs can be repaired through classic nonhomologous end joining (cNHEJ) allowing the two ends of the DSB to be re-ligated. (B) DSB ends can also be processed by the MRE11-RAD50-NBS1 (MRN) complex and its interacting factors to yield short 3′ single-strand (ss)DNA overhangs. (C) The short 3′ ssDNA overhangs can then be channeled into the microhomology-mediated end joining (MMEJ) pathway. (D) Alternatively, the DSB ends can undergo further long-range resection by either EXO1 or Bloom helicase (BLM)/DNA2. These longer ssDNA overhangs are first bound by replication protein A (RPA) and

(Figure legend continued at the bottom of the next page.)

We have a limited understanding of the factors that regulate the annealing of microhomologous sequences during MMEJ [11,76]. The ssDNA binding-protein replication protein A (**RPA**) can inhibit MMEJ by preventing annealing, whereas poly ADP-ribose polymerase 1 (PARP1) tethers DNA fragments together and promotes the annealing reaction [88–91]. However, there is conflicting evidence regarding the regulation of PARP1 in MMEJ [91,92]. Some studies suggest that PARP1 promotes MMEJ by competing with Ku for DSBs end binding [91], while other studies indicate that PARP1 promotes Ku loading [92]. In addition, pol θ can strip RPA from ssDNA to promote MMEJ [93]. Future studies will be essential to more fully understand how the interplay between these protein factors affect MMEJ.

If the microhomologous sequences are at the very ends of the DNA, then no further trimming is required [11]. By contrast, for microhomologies located distal to the DNA ends, the resulting heterologous 3′ ssDNA flap must be removed by XPF-ERCC1 endonuclease (called Rad1-Rad10 in *Saccharomyces cerevisiae*), or perhaps another unidentified nuclease, to allow a DNA polymerase to fill in the gap [94]. In mammalian cells, pol θ stabilizes annealed overhangs and fills any gaps via template-directed DNA synthesis [77,95]. Once the gaps are filled, the remaining nicks are sealed by DNA ligase III (LigIII) or DNA ligase I (LigI) [78].

Up to ~58% of Cas9-induced DSBs are repaired through MMEJ [96]. The resulting repair outcomes are not totally random and can be predicated at a given DSB site, indicating that the alignment between resected DNA ends at a given DSB site is reproducible and may depend on local sequence context [19,96–98]. Several lines of evidence suggest that deletion of two or more nucleotides at the Cas9 cut site is the most common outcome [19,96,98,99]. Inhibition of MMEJ decreases these nucleotide deletions significantly [100]. By taking advantage of this reproducible behavior, precise template-free genome editing through MMEJ has been achieved [96].

Single-Strand Annealing

SSA and MMEJ are similar in several aspects, in particular, they both require 3′ ssDNA overhangs for the annealing of homologous sequences [11,12]. Like MMEJ, SSA requires removal of heterologous 3′ flaps followed by gap filling [12].

SSA requires long-range DSB end resection to yield long (>1000 nucleotides) ssDNA overhangs (Figure 2D). These 3′ ssDNA overhangs are generated by the 5′ to 3′ exonuclease activities of either EXO1 or Bloom helicase (**BLM**)-DNA2 [80,101,102]. The resulting ssDNA overhangs are then coated by RPA, followed by the binding of RAD52, which mediates the annealing of homologous sequences within the two DSB ends (Figure 2E) [103–105]. In *S. cerevisiae*, Rad52 also stimulates the assembly of Rad51 filaments onto the ssDNA to promote HR (see later) [106]. By contrast, mammalian RAD52 does not stimulate **RAD51** filament assembly [105,107]. Indeed, the protein BRCA2 promotes RAD51 filament assembly in mammals, thus inhibiting SSA and favoring HR. In *S. cerevisiae*, Rad59 helps to channel repair intermediates through Rad52-mediated SSA by alleviating the inhibition of Rad51 on the strand annealing activity of Rad52 [108]. Although there is no mammalian Rad59 homolog, other factors (e.g., RAD52) that function similarly may exist [109]. Like MMEJ, the heterologous 3′ flap is removed by XPF-ERCC1 endonuclease during SSA [110]. However, details regarding how the gaps are filled and ligated remain uncertain [12,109].

can then be channeled into the (E) single-strand annealing (SSA) pathway, which is mediated by the protein RAD52. (F) Alternatively, the RPA-ssDNA can serve as a substrate for RAD51 filament assembly, allowing the resulting DNA intermediates to be directed towards repair by (G) homology repair (HR). For HR, both ssDNA and dsDNA templated homology-directed repair (HDR) pathways are shown. Abbreviations: CtIP, C-terminal binding protein interacting protein; DNA-PK, DNA-dependent protein kinase; XLF, XRCC4-like factor; XRCC4, X-ray cross complementing group 4.

Homologous Recombination

HR uses a homologous DNA template to guide DSB repair (Figure 2F,G) [9,81,109]. HR involves long-range end resection to form long 3′ ssDNA overhangs that are then coated by RPA (Figure 2D) [111]. RPA is replaced by the ATP-dependent DNA recombinase RAD51, which forms long helical filaments on the ssDNA (Figure 2F) [112,113]. RAD51 then aligns and pairs the ssDNA with homologous dsDNA elsewhere in the genome (Figure 2G). The 3′ invading end of the RAD51-coated ssDNA strand is used to prime DNA synthesis and the resulting intermediates can be used to complete repair of the DSB [9,81,109,114].

End Resection

End resection during HR requires two steps, beginning with MRN-CtIP mediated short-range resection (Figure 2B), followed by long-range end resection involving EXO1 and/or BLM/DNA2 (Figure 2D) [83,84,101,102]. Activation of key DNA end resection factors is strictly regulated by cell cycle and restricted mainly to the S/G2 phases of the cell cycle [82,115]. Several regulatory factors affect these DNA end resection steps.

Short-Range End Resection

MRN is crucial for short-range end resection and is controlled by numerous regulatory factors (Figure 2B) [116,117]. PARP1 is quickly recruited to new DSBs and can inhibit resection and recruit Ku to favor cNHEJ [92]. However, PARP1 can also facilitate MRN recruitment, which may favor MMEJ, SSA or HR [118]. Further studies are required to more fully understand these seemingly conflicting roles. DNA-PK also binds DNA ends and may commit cells to cNHEJ [10,109]. DNA-PK can be removed by phosphorylation of Ku70 to reduce its DNA-binding affinity [119], degradation of Ku through ubiquitination [120], or MRN-mediated DNA cleavage [121]. Removal of DNA-PK favors MMEJ, SSA, and HR [9,122]. DNA-PK can also promote MRN-mediated end processing, indicating that it plays a key role in initiating short-range end resection [121]. Phosphorylated CtIP and the breast cancer type 1 susceptibility protein–BRCA1-associated domain 1 (**BRCA1-BARD1**) complex both stimulate short-range end resection by MRN [84,123]. The recently discovered protein DYNLL1 (dynein light chain 1 protein) also inhibits MRN nuclease activity [124] and ZPET (zinc figure protein proximal to RAD18) delays MRN-CtIP recruitment through an unknown mechanism to inhibit the short-range end resection [125,126].

Long-Range End Resection

Short overhangs generated by MRN serve as an entry site for enzymes such as BLM/DNA2 or EXO1, which are necessary for long-range end resection (Figure 2D) [101,102]. EXO1 generates long 3′ ssDNA overhangs through its processive 5′ to 3′ exonuclease activity [102]. MRN stimulates EXO1, whereas CtIP inhibits EXO1 [102,127]. In mammalian cells, RPA can both stimulate and inhibit EXO1 activity (depending upon whether or not RPA is phosphorylated) [128], while SOSS1, the human SSB homologue 1, can stimulate resection by EXO1 [129].

BLM acts in concert with DNA2, which has both 5′ and 3′ endonuclease activities [128]. BLM separates the DNA strands, allowing DNA2 to cleave the ssDNA [102]. During long-range end resection, RPA inhibits the 3′ endonuclease activity of DNA2 while stimulating its 5′ endonuclease activity to ensure the 5′ to 3′ polarity of resection (Figure 2D) [130]. BLM/DNA2 loading at DNA ends is mediated by the TOPIIIα-RMI1-RMI2 complex and MRN [131]. CtIP also interacts with BLM and DNA2 and stimulates both BLM helicase activity and DNA2 5′ endonuclease activity [132].

Recent discoveries have revealed a regulatory mechanism involving 53BP1, PTIP, RIF1, and Shieldin-CST that inhibits end resection and a competing regulatory mechanism involving BARD1-BARD1 that promotes end resection [133–135]. In *S. cerevisiae*, Rad9 (a homolog of

human 53BP1) limits long-range resection [136]. Activated ATM at DSBs leads to histone H2AX phosphorylation, referred to as γH2AX, leading to MDC1 recruitment and phosphorylation [137]. Phosphorylated MDC1 recruits two E3 ubiquitin ligases, RNF8 and RNF168, to ubiquitinate histone H2A [138]. Ubiquitylated H2A together with H4K20me2 recruit 53BP1 to chromatin adjacent to the DSBs. Phosphorylated 53BP1 interacts with either PTIP or RIF1, both of which inhibit end resection albeit by different mechanisms [138]. The function of PTIP remains elusive [138], whereas RIF1 recruits the Shieldin complex (comprising SHLD1, SHLD2, SHLD3, and REV7) [133–135]. One model suggests that Shieldin binds at the DNA end to protect the 5′ end from end resection [133,135]. An alternative model suggests that Shieldin recruits CST, Polα, and Primase to DSBs [134]. CST binds at the dsDNA–ssDNA junction to protect the 5′ end and Polα and primase execute a fill-in reaction, which are stimulated by CST to counteract end resection [134].

BRCA1-BARD1 and 53BP1 may act in opposition to one another [139,140]. Current evidence suggests that BRCA1 prevents 53BP1 from inhibiting long-range resection and directly promotes long-range end resection [139]. 53BP1 blocks BRCA1 accumulation at DSBs during G1, whereas BRCA1 prevents 53BP1 and RIF1 foci formation at DSBs during S/G2 [126,139]. The antagonistic relationship between BRCA1-BARD1 and 53BP1 may be related to two histone (H2A and H4) post-translational modification states, lysine 15 ubiquitylation of H2A and lysine 20 methylation of H4 to effect DSB repair pathway choice [141]. In addition, BRCA1 can interact with MRN and CtIP to stimulate end resection during S/G2 [142].

RAD51 Filament Formation

The 3′ ssDNA overhang generated by long-range resection is first bound by RPA (Figure 2D) [111]. RPA must be replaced by RAD51, which is the recombinase that catalyzes key DNA transactions during HR (Figure 2F) [112,113]. However, RPA presents a barrier to RAD51 filament assembly [109,143]. During S/G2, RAD51 is phosphorylated by CDK1, which enhances its ability to compete with RPA for ssDNA [144]. However, RAD51 alone cannot efficiently replace RPA from ssDNA *in vivo* [143]. In *S. cerevisiae*, Rad52 stimulates Rad51 filament formation on RPA-bound ssDNA [106]. However human RAD52 does not fulfill a similar role [105,107]. Instead, human RAD51 filament assembly is facilitated by the BRCA2-DSS1 complex. BRCA1-BARD1 maybe also be involved in this process as part of a large complex with PALB2 and BRCA2–DSS1 [139,145].

Loss of the **RAD51 paralogs** BCDX2 or CX3 significantly reduces RAD51 foci formation in cells, indicating that both are required to promote RAD51 filament formation or stability [146]. Loss of SWS1 or SWSAP1, both components of the human Shu complex, also reduces RAD51 foci formation, although HR efficiency in these cells is comparable to wild-type [147]. These data all suggest roles for BCDX2, CX3, and the Shu complex during RAD51 filament formation, but underlying mechanisms remain unclear. DSS1 is a highly acidic protein that mimics DNA and directly interacts with RPA to weaken the affinity of RPA for ssDNA [148]. BRCA2 comprises an N-terminal DNA binding domain (NTD) which interacts with PALB2 [149], eight BRC repeats domain (BRC) that recruit RAD51 [150], a DNA binding domain (DBD) comprised of three OB folds to bind ssDNA [151], and an additional C-terminal RAD51-binding domain (CTRB) [152]. The SWI5-SFR1 complex also stabilizes RAD51 bound to ssDNA [153].

There are also negative regulatory factors that remove RAD51 from ssDNA [143]. In human cells, the helicases RECQ5, FBH1, and FANCJ downregulate HR by using the energy derived from ATP hydrolysis to translocate along ssDNA while stripping RAD51 from the ssDNA [143]. Similarly, the helicase FBH1 acts together with SCF ubiquitin ligase complex to ubiquitylate RAD51 causing RAD51 to relocate to the cytoplasm [154].

RAD51-Mediated Pairing of Homologous Sequences

RAD51, together with additional accessary factors, must align the ssDNA overhang with a homologous sequence that can be used to guide repair (Figure 2G). It must then invade the homologous dsDNA to form base-pairing interactions with the homologous template strand, resulting in the formation of a heteroduplex DNA joint (Figure 2G) [9,81,109,114]. Accessory factors that participate in this process, include RAD54, BRCA1-BARD1, PALB2, RAD51AP1-UAF1, and HOP2-MND1 [155–161]. *S. cerevisiae* Rad54 acts as a molecular motor to drive rapid ATP-dependent translocation of the RAD51 presynaptic filament along the dsDNA to facilitate sequence alignment and opens the dsDNA to facilitate strand invasion [155]. BRCA1-BARD1 and RAD51AP1-UAF1 promote the interaction between the RAD51 filament and the homologous dsDNA [156,157]. PALB2 stimulates RAD51 strand invasion activity through an unknown mechanism [158,159], although, its N-terminal DBD may play an important role [160]. HOP2-MND1 stabilizes RAD51 filaments and stimulates strand invasion [161].

DNA Synthesis and Product Resolution

After D-loop formation, the 3′ end of the invading strand is engaged by DNA polymerase δ (Polδ), PCNA, and clamp loader complex RFC1-5, allowing the broken DNA end to be extended using the homologous donor dsDNA as a template [9,81,109,114]. The resulting intermediates can be resolved through several mechanisms, including the non-crossover synthesis-dependent DNA strand annealing (SDSA), double Holliday junction (dHJ) crossover and non-crossover pathway and break-induced replication (BIR) (reviewed in [109,162,163]). BIR enables repair of just one of the two DSB ends and is not applicable to genome editing [163]. In SDSA, the heteroduplex DNA joint is disrupted by BLM, RTEL1, or another helicase [109,164,165] and can then be annealed with the other end of the DSB allowing for completion of repair by gap filling and ligation (Figure 2G) [109]. When both ends invade the same template, the interacting DNAs are joined by two Holliday junctions to form a dHJ (Figure 2G). dHJ can undergo dissolution to yield two intact dsDNA molecules [162]. In mammals, dHJ dissolution is catalyzed either by topoisomerase IIIα together with BLM-RMI1-RMI2 resulting in noncrossover products. Alternatively, dHJs can be resolved into cross-over products when cleaved by nucleases such as MUS81-EME1, SLX1-SLX4, and GEN1 [162].

Factors Affecting DNA Repair Outcomes of Cas9-Induced DSBs

Cas9-mediated genome editing outcomes depend on which DNA repair pathway is utilized. In this section, we summarize factors that can affect DNA repair outcomes of Cas9-induced DSBs and describe DNA repair outcomes of Cas9-induced DSBs.

Cell Cycle

The cell cycle is one of the most important factors affecting repair pathway choice [115,123,166,167]. cNHEJ is active across all stages of the cell-cycle, whereas SSA, MMEJ and HR function mainly during S/G2 (Figure 3A) [115,123,166,167]. Aphidicolin, which arrests cells in S/G2, promotes repair of Cas9-induced DSBs via SSA, MMEJ, and HR [168]. Fusing Cas9 to the protein Geminin, which is proteolytically degraded in G1, restricts Cas9 activity to S/G2 [169]. The recently developed technique of 'very fast CRISPR on demand', in which Cas9 prebinds to its target in genomic DNA in an inactive form and is activated by light to cleave the target DNA, can also be used to introduce DSBs when cells enter S/G2 [67].

Target Site Sequence and Chromatin Structure

DNA editing outcomes vary considerably among different genomic sites [97,98], but they are not completely arbitrary. For template-independent repair pathways (e.g., cNHEJ or MMEJ), the editing outcomes are significantly affected by the target site sequence (Figure 3B). A single protospacer targeting different genomic sites yielded similar repair events (Figure 3B) [99]. It

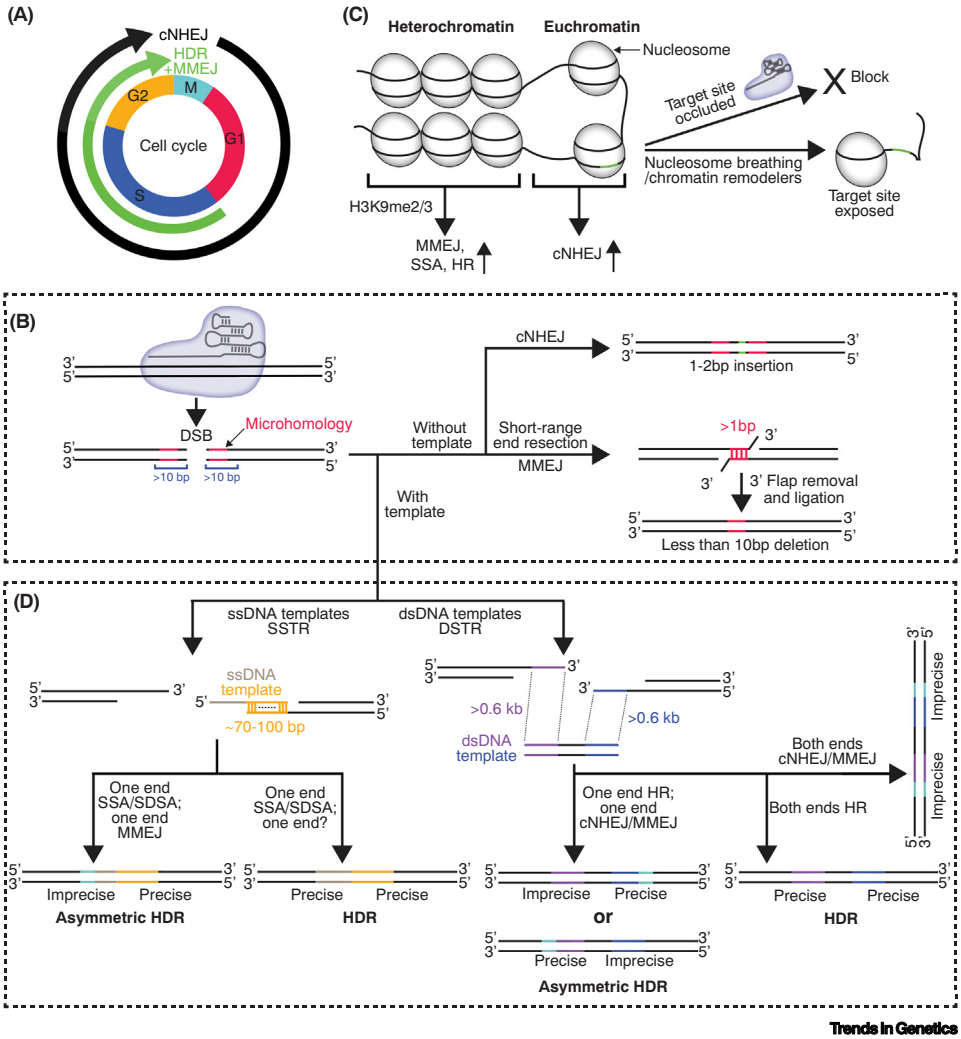

Trends in Genetics

Figure 3. Factors affecting DNA Repair Outcomes of Clustered Regularly Interspaced Short Palindromic Repeats-Associated Protein 9 (Cas9)-Induced Double-Strand Breaks (DSBs). (A) DSB repair pathways during the cell cycle. Classic nonhomologous end joining (cNHEJ) is active throughout the cell cycle (black circle). Microhomology-mediated end joining (MMEJ) and homology-directed repair (HDR) can only be used in S/G2 phases (green circle). (B) In the absence of a template guided repair mechanism editing outcomes are significantly affected by the target site sequence. MMEJ efficiency and the pattern of DNA small deletions are dependent upon the presence of microhomologies within the first 10 bp from the DSB end. One to 2 bp insertions/deletions through cNHEJ are affected by the nucleotide at the fourth position upstream from the protospacer adjacent motif (PAM). (C) Nucleosomes can potentially block Cas9 access to the target site, although sites can be exposed through nucleosome breathing or by a nucleosome remodeler. Compacted heterochromatin promotes homology repair (HR), MMEJ, and single-strand annealing (SSA), while cNHEJ is preferred in euchromatin. (D) Homology-directed repair (HDR) with single-strand (ss)DNA or double-strand (ds) DNA donor templates. dsDNA donor templated repair (DSTR) occurs mainly through HR and single-stranded DNA donor templated repair (SSTR) occurs mainly through SSA and SDSA. Asymmetric HDR can arise when one end is repaired through HR, while the other end is repaired through cNHEJ or MMEJ. With ssDNA, the end that is complementary to the 3′ end of ssDNA templates is repaired through SSA/synthesis-dependent DNA strand annealing (SDSA); it is not known how the other end is repaired. The repair of the other end through MMEJ generates asymmetric HDR which displays a bias directionality with respect to the orientation of the ssDNA templates.

has been shown that the nucleotides adjacent to the Cas9 cutting site can also affect editing outcomes [19,96–98]. The most common repair outcomes are small deletions (>3 bp) [96]. These small deletions are MMEJ products, indicating that microhomology adjacent to the cutting site

affects the deletion patterns (Figure 3B). Indeed, MMEJ efficiency and repair outcomes are significantly dependent on the microhomologies within the first 10 bp from the break [89]. Short 1–2 bp insertions/deletions are another common outcome and the relative percentage is affected by the nucleotide at the fourth position upstream from the PAM (see later) (Figure 3B) [96,170,171]. Thus, the sequence adjacent to the Cas9 cut site affects DSB repair.

Cas9 cleavage efficiency is also dependent on DNA accessibility (Figure 3C) [172]. Nucleosome breathing or changes in nucleosome architecture due to chromatin remodeling proteins can increase Cas9 cleavage efficiency (Figure 3C) [172]. Local chromatin structure also affects the choice of DSB repair pathways [173]. For example, histone post-translational modifications control recruitment of proteins such as 53BP1 and BRCA1, both of which influence DSB repair (Figure 3C) [174]. Heterochromatin and euchromatin also differentially affect DNA repair [174]. The H3K9 trimethylated (H3K9me2/3) marks present in heterochromatin promote HR, MMEJ, and SSA, while cNHEJ is preferred for euchromatin (Figure 3C) [173]. Detailed mechanisms of how local chromatin structure affects DNA repair pathways remain unclear and current studies are seeking to elucidate how chromatin structure affects Cas9-mediated genome editing [174].

Homology-Directed Repair with ssDNA or dsDNA Donor Templates

During CRISPR-Cas9 induced-DSB repair, template-dependent DSB repair pathways use an exogenous donor template to achieve precise gene editing [1]. Double-stranded DNA donor templated repair (DSTR) occurs mainly through the HR pathway, whereas single-stranded DNA donor templated repair (SSTR) occurs mainly through SSA and SDSA (synthesis dependent strand annealing) (Figure 3D) [13,175]. It has become clear that mis-integration events arise from MMEJ due to microhomologies within the DNA templates (Figure 3D) [175]. Thus, strategies that suppress MMEJ may improve both DSTR- and SSTR-based HDR.

For DSTR, the donor dsDNA can be either a PCR product or an exogenous plasmid [1]. For PCR products, mis-integration events arise mainly when the PCR products are ligated directly to a DSB through cNHEJ (Figure 3D) [175]. Inhibition of cNHEJ or 5′ covalent modification of the PCR products to prevent ligation can direct repair through HR [175]. In addition, a chromatin donor template is more efficient in D-loop formation than a naked DNA donor template *in vitro* [176]. *In vivo*, dsDNA donor templates coated with nucleosomes increase the frequency of DSTR-mediated HDR indicating that strategies which stimulate HR may be used to improve HDR [177]. For plasmid-based dsDNA templates, cells can incorporate the desired template along with the undesired plasmid backbone sequence into the genome [175]. Integration of the plasmid backbone is probably caused by asymmetric HDR which involves precise editing through HR on one side of a DSB and direct ligation through cNHEJ or MMEJ at the other side of the DSB (Figure 3D) [175]. Integration of the plasmid backbone might be reduced by transiently blocking cNHEJ or MMEJ [175]. Indeed, HDR can be improved by introducing two flanking Cas9 cleavage sites to excise the desired template from the plasmid backbone [178,179].

DSTR is more efficient than SSTR in *S. cerevisiae*, but SSTR- and DSTR-mediated genome editing occur with comparable efficiencies in mammalian cells [13]. SSTR is a more attractive option because short homology arms (around 70–100 bases compared with the 0.6–1.0 kb requirement for DSTR) can achieve efficient HDR and short ssDNA templates can be easily synthesized with multiple modifications to improve transformation efficiency and *in vivo* stability (Figure 3D) [180,181]. In *S. cerevisiae*, SSTR can be mediated through the SSA pathway and depends on Rad52, Rad59, antirecombinase Srs2, and MRX complex [108]. Thus, factors that inhibit SSA impair SSTR including Rad51, Rad57, and Rdh54 [108]. Similarly, SSTR in mammalian cells is also RAD51-independent and requires RAD52 [182]. RAD52 over-expression or fusion of RAD52 to Cas9

promotes SSTR mediated genome editing efficiency [182]. In addition to the SSA pathway, SDSA is also used during SSTR mediated DNA repair. Asymmetric HDR when using ssDNA donor templates is more prevalent than that of dsDNA donors and displays a bias with respect to the orientation of the targeted insertion (Figure 3D) [175]. These results may indicate that one end of the ssDNA donor is annealed to one of the DSB ends and repaired through SDSA or SSA, while the other end of the ssDNA donors may be repaired through non-HDR mechanism (Figure 3D) [175]. Although short ssDNA donor templates are more efficient than the dsDNA donor templates in promoting genome editing, long ssDNA donors induce more error-prone repair events than dsDNA donors because the microhomology sequences within long ssDNA donors generate truncations.

DNA Repair Outcomes of Cas9-Induced DSBs

As summarized earlier, cell cycle and end resection properties are important factors in determining DNA repair pathway choice between cNHEJ, MMEJ, SSA, and HR (Figures 2 and 3A). DNA repair outcomes are dependent on Cas9-induced DSB formation and detection time (Figure 4).

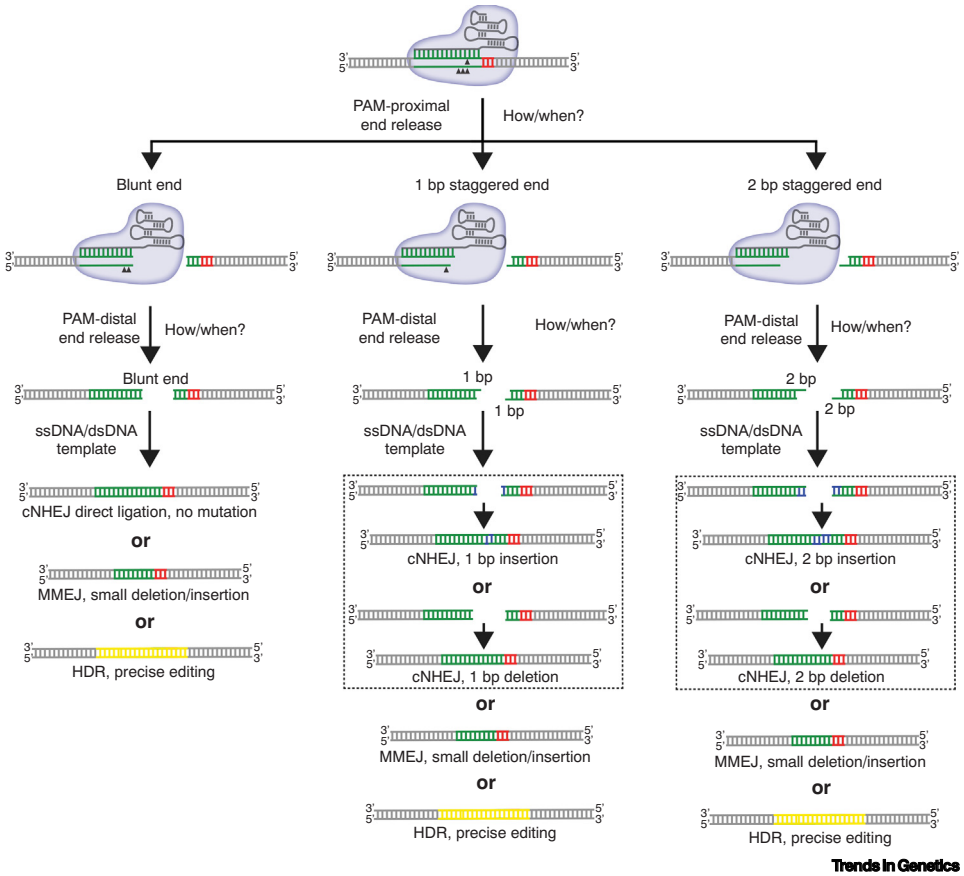

Figure 4. The Outcomes of Clustered Regularly Interspaced Short Palindromic Repeats-Associated Protein 9 (Cas9)-Induced DNA Double-Strand Break (DSB) Repair. Once the Cas9-guide (g)RNA complex binds to its target site, the HNH domain accurately cuts at the target strand –3 bp upstream of the protospacer-adjacent motif (PAM), while the RuvC-like domain cuts the –3, –4, or –5 positions of non-target strand. These cleavages can generate DSBs with either blunt ends or 1–2 nucleotide staggered ends. Blunt ends can be ligated directly through classic nonhomologous end joining (cNHEJ) without introducing any mutations, while staggered ends need to be filled or cleaved before ligation resulting 1–2 bp insertions or deletions. End resection directs DSB repair through template-independent microhomology-mediated end joining (MMEJ) or template-dependent homology-directed repair (HDR). For MMEJ, small homologous DNA sequences (5–25 bp) within the two resected ends are paired and lead to DNA repair resulting in small deletions or insertions. In the presence of either single-strand (ss)DNA or dsDNA templates, HDR compete with cNHEJ and MMEJ for precise DNA repair.

The time required for Cas9 to generate a DSB has been studied extensively and strategies have been developed to generate DSBs in S/G2 when HDR pathways function. However, the time required for the cell to detect a Cas9-induced DSB may be different from the time needed to detect a naturally occurring DSB. *In vitro*, Cas9 remains tightly bound for hours after cutting the DNA [15]. Delayed detection of Cas9-induced DSBs may influence the choice of DNA repair pathway (Figure 4) [68,170]. Although Cas9 dissociation is much faster *in vivo*, it still takes the cell at least 10 minutes to detect Cas9-induced DSBs, which is much longer than the time needed to detect normal DSBs [67]. Another study has suggested that Cas9 remains more tightly bound to the PAM-distal DSB end even after the proximal end is released [68]. Tight binding of Cas9 on the PAM-distal DSB end may alter repair kinetics and/or mechanism [170]. Factors such as RNA-polymerase and the histone chaperone FACT promote Cas9 release and may affect DNA repair outcomes [68,69]. cNHEJ is the major repair pathway to repair ionizing radiation (IR) induced DSBs and MMEJ is less efficient [183]. However, MMEJ is improved at least twofold for Cas9 induced DSBs [170]. Indeed, up to 58% of Cas9-induced DSBs can be repaired through MMEJ [96]. These results indicate the possibility that the asymmetric release of Cas9-induced DSB ends may somehow enhance MMEJ while disfavoring cNHEJ.

DSB ends generated by Cas9 are either blunt or have a 1–2 bp staggered 5′ end (Figure 4) [19]. Blunt ends can be ligated directly by the LigIV-XRCC4-XLF complex through cNHEJ (Figure 4A), while staggered ends require further processing (Figure 4B,C)[184]. cNHEJ is a major pathway used to repair the 5′ staggered ends, resulting in 1–2 bp insertions or deletions (Figure 4) [96]. The 1–2 bp staggered ends may be filled in by a polymerase or removed by a nuclease to create a blunt end, followed by ligation through cNHEJ (Figure 4A)[184]. In addition, we speculate that the 5′ staggered ends slow cNHEJ repair kinetics long enough for cells to initiate MMEJ, SSA, or HR (Figure 3D).

Increasing evidence has suggested that large deletions can happen at on-target sites during CRISPR-Cas9 editing [185–187]. Current evidence suggests that large deletions are mainly caused by the DSBs generated by CRISPR-Cas9 in a p53-dependent mechanism [188]. Although the frequency of large deletion events is very low, they may cause serious problems. Thus, studies to elucidate how large deletions are generated could be highly beneficial.

Outstanding Questions

After cleavage, Cas9 asymmetrically releases the PAM-proximal end of the DSB within minutes. How is this achieved? How is the PAM-proximal end of the DSB released? How long does Cas9 remain bound to the PAM-distal end of the DSB after the PAM-proximal end is released? How is the PAM-distal end of the DSB released? How might asymmetric release of Cas9 from a DSB affect repair pathway choice?

Long-range end resection commits DSB repair to the HR and SSA pathways. How is end resection regulated by BRCA1-BARD1, 53BP1, and the Shieldin complex? What is the temporal recruitment order of these regulators?

For SSTR, how do mammalian cells choose between the SSA and SDSA pathways? What is the relative contribution of each pathway to repair? Do other pathways also contribute to SSTR?

How do DNA templates in the cytosol enter the nucleus? How do foreign DNA sensing pathways, including TLR9, AIM2, and cGAS, affect genome editing? Is it possible to transiently inhibit foreign DNA sensing pathways during template delivery?

Concluding Remarks

It is important to recognize that CRISPR-Cas-based genome editing depends on the four major DSB repair pathways found in eukaryotic cells. Different pathways result in different editing outcomes. Hence, efforts are being made to control which pathways cell utilize to repair DSBs during genome editing (see Outstanding Questions). However, the mechanisms that control DSB repair are themselves highly complex and are not yet fully understood [9–12,115,123,166,167,174]. Understanding DSB repair mechanisms will yield fundamental insights into genome integrity and will help establish better genome editing strategies.

Acknowledgments

We apologize to colleagues whose work could not be cited because of space constraints. We thank Samuel H. Sternberg, Alberto Ciccia, Upasana Roy, and Aviv Meir for their critical reading of the manuscript. The Greene laboratory is supported by funding from the National Institutes of Health (R35GM118026, R01CA236606, and R01CA221858) and the National Science Foundation (MCB1817315).

Declaration of Interests

None declared by authors.

References

1. Doudna, J.A. and Charpentier, E. (2014) Genome editing. The new frontier of genome engineering with CRISPR-Cas9. *Science* 346, 1258096
2. Urnov, F.D. *et al.* (2010) Genome editing with engineered zinc finger nucleases. *Nat. Rev. Genet.* 11, 636–646
3. Miller, J.C. *et al.* (2011) A TALE nuclease architecture for efficient genome editing. *Nat. Biotechnol.* 29, 143–148
4. Jinek, M. *et al.* (2012) A programmable dual-RNA-guided DNA endonuclease in adaptive bacterial immunity. *Science* 337, 816–821
5. Jinek, M. *et al.* (2013) RNA-programmed genome editing in human cells. *eLife* 2, e00471
6. Cong, L. *et al.* (2013) Multiplex genome engineering using CRISPR/Cas systems. *Science* 339, 819–823
7. Mali, P. *et al.* (2013) RNA-guided human genome engineering via Cas9. *Science* 339, 823–826
8. Gasiunas, G. *et al.* (2012) Cas9-crRNA ribonucleoprotein complex mediates specific DNA cleavage for adaptive immunity in bacteria. *Proc. Natl. Acad. Sci. U. S. A.* 109, E2579–E2586
9. Sung, P. and Klein, H. (2006) Mechanism of homologous recombination: mediators and helicases take on regulatory functions. *Nat. Rev. Mol. Cell Biol.* 7, 739–750
10. Chang, H.H.Y. *et al.* (2017) Non-homologous DNA end joining and alternative pathways to double-strand break repair. *Nat. Rev. Mol. Cell Biol.* 18, 495–506
11. Sfeir, A. and Symington, L.S. (2015) Microhomology-mediated end joining: A back-up survival mechanism or dedicated pathway? *Trends Biochem. Sci.* 40, 701–714
12. Bhargava, R. *et al.* (2016) Regulation of single-strand annealing and its role in genome maintenance. *Trends Genet.* 32, 566–575
13. Yeh, C.D. *et al.* (2019) Advances in genome editing through control of DNA repair pathways. *Nat. Cell Biol.* 21, 1468–1478
14. Chen, H. *et al.* (2014) Cut site selection by the two nuclease domains of the Cas9 RNA-guided endonuclease. *J. Biol. Chem.* 289, 13284–13294
15. Sternberg, S.H. *et al.* (2014) DNA interrogation by the CRISPR RNA-guided endonuclease Cas9. *Nature* 507, 62–67
16. Szczelkun, M.D. *et al.* (2014) Direct observation of R-loop formation by single RNA-guided Cas9 and Cascade effector complexes. *Proc. Natl. Acad. Sci. U. S. A.* 111, 9798–9803
17. Chen, J.S. *et al.* (2017) Enhanced proofreading governs CRISPR-Cas9 targeting accuracy. *Nature* 550, 407–410
18. Dagdas, Y.S. *et al.* (2017) A conformational checkpoint between DNA binding and cleavage by CRISPR-Cas9. *Sci. Adv.* 3, eaao0027
19. Shou, J. *et al.* (2018) Precise and predictable CRISPR chromosomal rearrangements reveal principles of Cas9-mediated nucleotide insertion. *Mol. Cell* 71, 498–509 e4
20. Pattanayak, V. *et al.* (2013) High-throughput profiling of off-target DNA cleavage reveals RNA-programmed Cas9 nuclease specificity. *Nat. Biotechnol.* 31, 839–843
21. Fu, Y. *et al.* (2013) High-frequency off-target mutagenesis induced by CRISPR-Cas nucleases in human cells. *Nat. Biotechnol.* 31, 822–826
22. Kuscu, C. *et al.* (2014) Genome-wide analysis reveals characteristics of off-target sites bound by the Cas9 endonuclease. *Nat. Biotechnol.* 32, 677–683
23. Slaymaker, I.M. *et al.* (2016) Rationally engineered Cas9 nucleases with improved specificity. *Science* 351, 84–88
24. Kleinstiver, B.P. *et al.* (2016) High-fidelity CRISPR-Cas9 nucleases with no detectable genome-wide off-target effects. *Nature* 529, 490–495
25. Lee, J.K. *et al.* (2018) Directed evolution of CRISPR-Cas9 to increase its specificity. *Nat. Commun.* 9, 3048
26. Vakulskas, C.A. *et al.* (2018) A high-fidelity Cas9 mutant delivered as a ribonucleoprotein complex enables efficient gene editing in human hematopoietic stem and progenitor cells. *Nat. Med.* 24, 1216–1224
27. Yin, H. *et al.* (2017) Delivery technologies for genome editing. *Nat. Rev. Drug Discov.* 16, 387–399
28. Senis, E. *et al.* (2014) CRISPR/Cas9-mediated genome engineering: an adeno-associated viral (AAV) vector toolbox. *Biotechnol. J.* 9, 1402–1412
29. Wang, D. *et al.* (2015) Adenovirus-mediated somatic genome editing of *Pten* by CRISPR/Cas9 in mouse liver in spite of Cas9-specific immune responses. *Hum. Gene Ther.* 26, 432–442
30. Genovese, P. *et al.* (2014) Targeted genome editing in human repopulating haematopoietic stem cells. *Nature* 510, 235–240
31. Yang, Y. *et al.* (2016) A dual AAV system enables the Cas9-mediated correction of a metabolic liver disease in newborn mice. *Nat. Biotechnol.* 34, 334–338
32. Ramakrishna, S. *et al.* (2014) Gene disruption by cell-penetrating peptide-mediated delivery of Cas9 protein and guide RNA. *Genome Res.* 24, 1020–1027
33. Hendel, A. *et al.* (2015) Chemically modified guide RNAs enhance CRISPR-Cas genome editing in human primary cells. *Nat. Biotechnol.* 33, 985–989
34. Rahdar, M. *et al.* (2015) Synthetic CRISPR RNA-Cas9-guided genome editing in human cells. *Proc. Natl. Acad. Sci. U. S. A.* 112, E7110–E7117
35. Heil, F. *et al.* (2004) Species-specific recognition of single-stranded RNA via toll-like receptor 7 and 8. *Science* 303, 1526–1529
36. Hornung, V. *et al.* (2005) Sequence-specific potent induction of IFN-alpha by short interfering RNA in plasmacytoid dendritic cells through TLR7. *Nat. Med.* 11, 263–270
37. Wang, X. *et al.* (2015) Unbiased detection of off-target cleavage by CRISPR-Cas9 and TALENs using integrase-defective lentiviral vectors. *Nat. Biotechnol.* 33, 175–178
38. Yin, H. *et al.* (2016) Therapeutic genome editing by combined viral and non-viral delivery of CRISPR system components in vivo. *Nat. Biotechnol.* 34, 328–333
39. Wang, M. *et al.* (2016) Efficient delivery of genome-editing proteins using bioreducible lipid nanoparticles. *Proc. Natl. Acad. Sci. U. S. A.* 113, 2868–2873
40. Shahbazi, R. *et al.* (2019) Targeted homology-directed repair in blood stem and progenitor cells with CRISPR nanoformulations. *Nat. Mater.* 18, 1124–1132
41. Silva, G. *et al.* (2011) Meganucleases and other tools for targeted genome engineering: perspectives and challenges for gene therapy. *Curr. Gene Ther.* 11, 11–27
42. Schumann, K. *et al.* (2015) Generation of knock-in primary human T cells using Cas9 ribonucleoproteins. *Proc. Natl. Acad. Sci. U. S. A.* 112, 10437–10442
43. Holkers, M. *et al.* (2014) Adenoviral vector DNA for accurate genome editing with engineered nucleases. *Nat. Methods* 11, 1051–1057
44. Kim, S. *et al.* (2014) Highly efficient RNA-guided genome editing in human cells via delivery of purified Cas9 ribonucleoproteins. *Genome Res.* 24, 1012–1019
45. Hemmi, H. *et al.* (2000) A Toll-like receptor recognizes bacterial DNA. *Nature* 408, 740–745
46. Hornung, V. *et al.* (2009) AIM2 recognizes cytosolic dsDNA and forms a caspase-1-activating inflammasome with ASC. *Nature* 458, 514–518
47. Fernandes-Alnemri, T. *et al.* (2009) AIM2 activates the inflammasome and cell death in response to cytoplasmic DNA. *Nature* 458, 509–513
48. Burckstummer, T. *et al.* (2009) An orthogonal proteomic-genomic screen identifies AIM2 as a cytoplasmic DNA sensor for the inflammasome. *Nat. Immunol.* 10, 266–272
49. Lino, C.A. *et al.* (2018) Delivering CRISPR: a review of the challenges and approaches. *Drug Deliv.* 25, 1234–1257
50. Gori, J.L. *et al.* (2015) Delivery and specificity of CRISPR-Cas9 genome editing technologies for human gene therapy. *Hum. Gene Ther.* 26, 443–451
51. Sheng Tong, B.M. *et al.* (2019) Engineered materials for in vivo delivery of genome-editing machinery. *Nat. Rev. Mater.* 4, 726–737
52. Hirakawa, M.P. *et al.* (2020) Gene editing and CRISPR in the clinic: current and future perspectives. *Biosci. Rep.* 40, BSR20200127
53. Anzalone, A.V. *et al.* (2020) Genome editing with CRISPR-Cas nucleases, base editors, transposases and prime editors. *Nat. Biotechnol.* 38, 824–844
54. Zetsche, B. *et al.* (2015) Cpf1 is a single RNA-guided endonuclease of a class 2 CRISPR-Cas system. *Cell* 163, 759–771

55. Kleinstiver, B.P. *et al.* (2016) Genome-wide specificities of CRISPR-Cas Cpf1 nucleases in human cells. *Nat. Biotechnol.* 34, 869–874
56. Kim, D. *et al.* (2016) Genome-wide analysis reveals specificities of Cpf1 endonucleases in human cells. *Nat. Biotechnol.* 34, 863–868
57. Murugan, K. *et al.* (2020) CRISPR-Cas12a has widespread off-target and dsDNA-nicking effects. *J. Biol. Chem.* 295, 5538–5553
58. Fuchs, R.T. *et al.* (2019) Cas12a trans-cleavage can be modulated in vitro and is active on ssDNA, dsDNA, and RNA. *bioRxiv* Published online April 8, 2019. http://dx.doi.org/10.1101/600890
59. Spagnolo, L. *et al.* (2006) Three-dimensional structure of the human DNA-PKcs/Ku70/Ku80 complex assembled on DNA and its implications for DNA DSB repair. *Mol. Cell* 22, 51151–51159
60. Meek, K. *et al.* (2008) DNA-PK: the means to justify the ends? *Adv. Immunol.* 99, 33–58
61. Nick McElhinny, S.A. *et al.* (2000) Ku recruits the XRCC4-ligase IV complex to DNA ends. *Mol. Cell. Biol.* 20, 2996–3003
62. Andres, S.N. *et al.* (2007) Crystal structure of human XLF: a twist in nonhomologous DNA end-joining. *Mol. Cell* 28, 1093–1101
63. Mari, P.O. *et al.* (2006) Dynamic assembly of end-joining complexes requires interaction between Ku70/80 and XRCC4. *Proc. Natl. Acad. Sci. U. S. A.* 103, 18597–18602
64. Niewolik, D. *et al.* (2006) DNA-PKcs dependence of Artemis endonucleolytic activity, differences between hairpins and 5′ or 3′ overhangs. *J. Biol. Chem.* 281, 33900–33909
65. Niewolik, D. *et al.* (2017) Autoinhibition of the nuclease ARTEMIS is mediated by a physical interaction between its catalytic and C-terminal domains. *J. Biol. Chem.* 292, 3351–3365
66. Bernstein, N.K. *et al.* (2005) The molecular architecture of the mammalian DNA repair enzyme, polynucleotide kinase. *Mol. Cell* 17, 657–670
67. Liu, Y. *et al.* (2020) Very fast CRISPR on demand. *Science* 368, 1265–1269
68. Clarke, R. *et al.* (2018) Enhanced bacterial immunity and mammalian genome editing via RNA-polymerase-mediated dislodging of Cas9 from double-strand DNA breaks. *Mol. Cell* 71, 42–55
69. Wang, A.S. *et al.* (2020) The histone chaperone FACT induces Cas9 multi-turnover behavior and modifies genome manipulation in human cells. *Mol. Cell* 79, 221–233
70. Maruyama, T. *et al.* (2015) Increasing the efficiency of precise genome editing with CRISPR-Cas9 by inhibition of nonhomologous end joining. *Nat. Biotechnol.* 33, 538–542
71. Hu, Z. *et al.* (2018) Ligase IV inhibitor SCR7 enhances gene editing directed by CRISPR-Cas9 and ssODN in human cancer cells. *Cell Biosci.* 8, 12
72. Chu, V.T. *et al.* (2015) Increasing the efficiency of homology-directed repair for CRISPR-Cas9-induced precise gene editing in mammalian cells. *Nat. Biotechnol.* 33, 543–548
73. Ninomiya, Y. *et al.* (2004) Highly efficient gene replacements in *Neurospora* strains deficient for nonhomologous end-joining. *Proc. Natl. Acad. Sci. U. S. A.* 101, 12248–12253
74. Riesenberg, S. and Maricic, T. (2018) Targeting repair pathways with small molecules increases precise genome editing in pluripotent stem cells. *Nat. Commun.* 9, 2164
75. Robert, F. *et al.* (2015) Pharmacological inhibition of DNA-PK stimulates Cas9-mediated genome editing. *Genome Med.* 7, 93
76. Seol, J.H. *et al.* (2018) Microhomology-mediated end joining: Good, bad and ugly. *Mutat. Res.* 809, 81–87
77. Kent, T. *et al.* (2015) Mechanism of microhomology-mediated end-joining promoted by human DNA polymerase theta. *Nat. Struct. Mol. Biol.* 22, 230–237
78. Liang, L. *et al.* (2008) Human DNA ligases I and III, but not ligase IV, are required for microhomology-mediated end joining of DNA double-strand breaks. *Nucleic Acids Res.* 36, 3297–3310
79. Truong, L.N. *et al.* (2013) Microhomology-mediated end joining and homologous recombination share the initial end resection step to repair DNA double-strand breaks in mammalian cells. *Proc. Natl. Acad. Sci. U. S. A.* 110, 7720–7725
80. Symington, L.S. and Gautier, J. (2011) Double-strand break end resection and repair pathway choice. *Annu. Rev. Genet.* 45, 247–271
81. Ceccaldi, R. *et al.* (2016) Repair pathway choices and consequences at the double-strand break. *Trends Cell Biol.* 26, 52–64
82. Lee, J.H. and Paull, T.T. (2004) Direct activation of the ATM protein kinase by the Mre11/Rad50/Nbs1 complex. *Science* 304, 93–96
83. Sartori, A.A. *et al.* (2007) Human CtIP promotes DNA end resection. *Nature* 450, 509–514
84. Anand, R. *et al.* (2016) Phosphorylated CtIP functions as a co-factor of the MRE11-RAD50-NBS1 endonuclease in DNA end resection. *Mol. Cell* 64, 940–950
85. Myler, L.R. *et al.* (2017) Single-molecule imaging reveals how Mre11-Rad50-Nbs1 initiates DNA break repair. *Mol. Cell* 67, 891–898
86. Paull, T.T. and Gellert, M. (1998) The 3′ to 5′ exonuclease activity of Mre 11 facilitates repair of DNA double-strand breaks. *Mol. Cell* 1, 969–979
87. Srivastava, M. *et al.* (2012) An inhibitor of nonhomologous end-joining abrogates double-strand break repair and impedes cancer progression. *Cell* 151, 1474–1487
88. Deng, S.K. *et al.* (2014) RPA antagonizes microhomology-mediated repair of DNA double-strand breaks. *Nat. Struct. Mol. Biol.* 21, 405–412
89. Villarreal, D.D. *et al.* (2012) Microhomology directs diverse DNA break repair pathways and chromosomal translocations. *PLoS Genet.* 8, e1003026
90. Audebert, M. *et al.* (2004) Involvement of poly(ADP-ribose) polymerase-1 and XRCC1/DNA ligase III in an alternative route for DNA double-strand breaks rejoining. *J. Biol. Chem.* 279, 55117–55126
91. Wang, M. *et al.* (2006) PARP-1 and Ku compete for repair of DNA double strand breaks by distinct NHEJ pathways. *Nucleic Acids Res.* 34, 6170–6182
92. Caron, M.C. *et al.* (2019) Poly(ADP-ribose) polymerase-1 antagonizes DNA resection at double-strand breaks. *Nat. Commun.* 10, 2954
93. Mateos-Gomez, P.A. *et al.* (2017) The helicase domain of Polθ counteracts RPA to promote alt-NHEJ. *Nat. Struct. Mol. Biol.* 24, 1116–1123
94. Ahmad, A. *et al.* (2008) ERCC1-XPF endonuclease facilitates DNA double-strand break repair. *Mol. Cell. Biol.* 28, 5082–5092
95. Mateos-Gomez, P.A. *et al.* (2015) Mammalian polymerase theta promotes alternative NHEJ and suppresses recombination. *Nature* 518, 254–257
96. Shen, M.W. *et al.* (2018) Predictable and precise template-free CRISPR editing of pathogenic variants. *Nature* 563, 646–651
97. Chakrabarti, A.M. *et al.* (2019) Target-specific precision of CRISPR-mediated genome editing. *Mol. Cell* 73, 699–713
98. Allen, F. *et al.* (2018) Predicting the mutations generated by repair of Cas9-induced double-strand breaks. *Nat. Biotechnol.* 64–72
99. van Overbeek, M. *et al.* (2016) DNA repair profiling reveals nonrandom outcomes at Cas9-mediated breaks. *Mol. Cell* 63, 633–646
100. Iyer, S. *et al.* (2019) Precise therapeutic gene correction by a simple nuclease-induced double-stranded break. *Nature* 568, 561–565
101. Sturzenegger, A. *et al.* (2014) DNA2 cooperates with the WRN and BLM RecQ helicases to mediate long-range DNA end resection in human cells. *J. Biol. Chem.* 289, 27314–27326
102. Nimonkar, A.V. *et al.* (2011) BLM-DNA2-RPA-MRN and EXO1-BLM-RPA-MRN constitute two DNA end resection machineries for human DNA break repair. *Genes Dev.* 25, 350–362
103. Mortensen, U.H. *et al.* (1996) DNA strand annealing is promoted by the yeast Rad52 protein. *Proc. Natl. Acad. Sci. U. S. A.* 93, 10729–10734
104. Grimme, J.M. *et al.* (2010) Human Rad52 binds and wraps single-stranded DNA and mediates annealing via two hRad52-ssDNA complexes. *Nucleic Acids Res.* 38, 2917–2930

105. Ma, C.J. *et al.* (2017) Human RAD52 interactions with replication protein A and the RAD51 presynaptic complex. *J. Biol. Chem.* 292, 11702–11713
106. Sung, P. (1997) Function of yeast Rad52 protein as a mediator between replication protein A and the Rad51 recombinase. *J. Biol. Chem.* 272, 28194–28197
107. Feng, Z. *et al.* (2011) Rad52 inactivation is synthetically lethal with BRCA2 deficiency. *Proc. Natl. Acad. Sci. U. S. A.* 108, 686–691
108. Gallagher, D.N. *et al.* (2020) A Rad51-independent pathway promotes single-strand template repair in gene editing. *PLoS Genet.* 16, e1008689
109. Scully, R. *et al.* (2019) DNA double-strand break repair-pathway choice in somatic mammalian cells. *Nat. Rev. Mol. Cell Biol.* 20, 698–714
110. Al-Minawi, A.Z. *et al.* (2008) The ERCC1/XPF endonuclease is required for efficient single-strand annealing and gene conversion in mammalian cells. *Nucleic Acids Res.* 36, 1–9
111. Chen, H. *et al.* (2013) RPA coordinates DNA end resection and prevents formation of DNA hairpins. *Mol. Cell* 50, 589–600
112. Shrivastav, M. *et al.* (2008) Regulation of DNA double-strand break repair pathway choice. *Cell Res.* 18, 134–147
113. Xu, J. *et al.* (2017) Cryo-EM structures of human RAD51 recombinase filaments during catalysis of DNA-strand exchange. *Nat. Struct. Mol. Biol.* 24, 40–46
114. Kowalczykowski, S.C. (2015) An overview of the molecular mechanisms of recombinational DNA repair. *Cold Spring Harb. Perspect. Biol.* 7, a016410
115. Peterson, S.E. *et al.* (2011) Cdk1 uncouples CtIP-dependent resection and Rad51 filament formation during M-phase double-strand break repair. *J. Cell Biol.* 194, 705–720
116. Lamarche, B.J. *et al.* (2010) The MRN complex in double-strand break repair and telomere maintenance. *FEBS Lett.* 584, 3682–3695
117. Syed, A. and Tainer, J.A. (2018) The MRE11-RAD50-NBS1 complex conducts the orchestration of damage signaling and outcomes to stress in DNA replication and repair. *Annu. Rev. Biochem.* 87, 263–294
118. Haince, J.F. *et al.* (2008) PARP1-dependent kinetics of recruitment of MRE11 and NBS1 proteins to multiple DNA damage sites. *J. Biol. Chem.* 283, 1197–1208
119. Lee, K.J. *et al.* (2016) Phosphorylation of Ku dictates DNA double-strand break (DSB) repair pathway choice in S phase. *Nucleic Acids Res.* 44, 1732–1745
120. Jiang, N. *et al.* (2013) Valosin-containing protein regulates the proteasome-mediated degradation of DNA-PKcs in glioma cells. *Cell Death Dis.* 4, e647
121. Deshpande, R.A. *et al.* (2020) DNA-dependent protein kinase promotes DNA end processing by MRN and CtIP. *Sci. Adv.* 6, eaay0922
122. Allen, C. *et al.* (2002) DNA-dependent protein kinase suppresses double-strand break-induced and spontaneous homologous recombination. *Proc. Natl. Acad. Sci. U. S. A.* 99, 3758–3763
123. Yun, M.H. and Hiom, K. (2009) CtIP-BRCA1 modulates the choice of DNA double-strand-break repair pathway throughout the cell cycle. *Nature* 459, 460–463
124. He, Y.J. *et al.* (2018) DYNLL1 binds to MRE11 to limit DNA end resection in BRCA1-deficient cells. *Nature* 563, 522–526
125. Moquin, D.M. *et al.* (2019) Localized protein biotinylation at DNA damage sites identifies ZPET, a repressor of homologous recombination. *Genes Dev.* 33, 75–89
126. Ronato, D.A. *et al.* (2020) Limiting the DNA double-strand break resectosome for genome protection. *Trends Biochem. Sci.* 45, 779–793
127. Eid, W. *et al.* (2010) DNA end resection by CtIP and exonuclease 1 prevents genomic instability. *EMBO Rep.* 11, 962–968
128. Symington, L.S. (2016) Mechanism and regulation of DNA end resection in eukaryotes. *Crit. Rev. Biochem. Mol. Biol.* 51, 195–212
129. Myler, L.R. *et al.* (2016) Single-molecule imaging reveals the mechanism of Exo1 regulation by single-stranded DNA binding proteins. *Proc. Natl. Acad. Sci. U. S. A.* 113, E1170–E1179
130. Zhou, C. *et al.* (2015) Dna2 nuclease-helicase structure, mechanism and regulation by Rpa. *eLife* 4, e09832
131. Daley, J.M. *et al.* (2014) Multifaceted role of the Topo IIIalpha-RMI1-RMI2 complex and DNA2 in the BLM-dependent pathway of DNA break end resection. *Nucleic Acids Res.* 42, 11083–11091
132. Daley, J.M. *et al.* (2017) Enhancement of BLM-DNA2-mediated long-range DNA end resection by CtIP. *Cell Rep.* 21, 324–332
133. Gupta, R. *et al.* (2018) DNA repair network analysis reveals shieldin as a key regulator of NHEJ and PARP inhibitor sensitivity. *Cell* 173, 972–988 e23
134. Mirman, Z. *et al.* (2018) 53BP1-RIF1-shieldin counteracts DSB resection through CST- and Polalpha-dependent fill-in. *Nature* 560, 112–116
135. Noordermeer, S.M. *et al.* (2018) The shieldin complex mediates 53BP1-dependent DNA repair. *Nature* 560, 117–121
136. Ferrari, M. *et al.* (2020) Rad9/53BP1 promotes DNA repair via crossover recombination by limiting the Sgs1 and Mph1 helicases. *Nat. Commun.* 11, 3181
137. Lou, Z. *et al.* (2003) MDC1 is coupled to activated CHK2 in mammalian DNA damage response pathways. *Nature* 421, 957–961
138. Mirman, Z. and de Lange, T. (2020) 53BP1: a DSB escort. *Genes Dev.* 34, 7–23
139. Tarsounas, M. and Sung, P. (2020) The antitumorigenic roles of BRCA1-BARD1 in DNA repair and replication. *Nat. Rev. Mol. Cell Biol.* 21, 284–299
140. Bunting, S.F. *et al.* (2010) 53BP1 inhibits homologous recombination in Brca1-deficient cells by blocking resection of DNA breaks. *Cell* 141, 243–254
141. Becker, J.R. *et al.* (2020) BARD1 links histone H2A Lysine-15 ubiquitination to initiation of BRCA1-dependent homologous recombination. *bioRxiv* Published online June 1, 2020. https://doi.org/10.1101/2020.06.01.127951
142. Chen, L. *et al.* (2008) Cell cycle-dependent complex formation of BRCA1.CtIP.MRN is important for DNA double-strand break repair. *J. Biol. Chem.* 283, 7713–7720
143. Bonilla, B. *et al.* (2020) RAD51 gene family structure and function. *Annu. Rev. Genet.* 54, 25–46
144. Lim, G. *et al.* (2020) Phosphoregulation of Rad51/Rad52 by CDK1 functions as a molecular switch for cell cycle-specific activation of homologous recombination. *Sci. Adv.* 6, eaay2669
145. Chen, C.C. *et al.* (2018) Homology-directed repair and the role of BRCA1, BRCA2, and related proteins in genome integrity and cancer. *Annu. Rev. Cancer Biol.* 2, 313–336
146. Garcin, E.B. *et al.* (2019) Differential requirements for the RAD51 paralogs in genome repair and maintenance in human cells. *PLoS Genet.* 15, e1008355
147. Prakash, R. *et al.* (2020) Distinct pathways of homologous recombination controlled by the SWS1-SWSAP1-SPIDR complex. *bioRxiv* Published online May 15, 2020. http://dx.doi.org/10.1101/2020.05.15.098848
148. Zhao, W. *et al.* (2015) Promotion of BRCA2-dependent homologous recombination by DSS1 via RPA targeting and DNA mimicry. *Mol. Cell* 59, 176–187
149. Xia, B. *et al.* (2006) Control of BRCA2 cellular and clinical functions by a nuclear partner, PALB2. *Mol. Cell* 22, 719–729
150. Chen, P.L. *et al.* (1998) The BRC repeats in BRCA2 are critical for RAD51 binding and resistance to methyl methanesulfonate treatment. *Proc. Natl. Acad. Sci. U. S. A.* 95, 5287–5292
151. Yang, H. *et al.* (2002) BRCA2 function in DNA binding and recombination from a BRCA2-DSS1-ssDNA structure. *Science* 297, 1837–1848
152. Sharan, S.K. *et al.* (1997) Embryonic lethality and radiation hypersensitivity mediated by Rad51 in mice lacking Brca2. *Nature* 386, 804–810
153. Lu, C.H. *et al.* (2018) Swi5-Sfr1 stimulates Rad51 recombinase filament assembly by modulating Rad51 dissociation. *Proc. Natl. Acad. Sci. U. S. A.* 115, E10059–E10068
154. Chu, W.K. *et al.* (2015) FBH1 influences DNA replication fork stability and homologous recombination through ubiquitylation of RAD51. *Nat. Commun.* 6, 5931
155. Crickard, J.B. *et al.* (2020) Rad54 drives ATP hydrolysis-dependent DNA sequence alignment during homologous recombination. *Cell* 181, 1380–1394 e18
156. Zhao, W. *et al.* (2017) BRCA1-BARD1 promotes RAD51-mediated homologous DNA pairing. *Nature* 550, 360–365

157. Liang, F. *et al.* (2016) Promotion of RAD51-mediated homologous DNA pairing by the RAD51AP1-UAF1 complex. *Cell Rep.* 15, 2118–2126
158. Dray, E. *et al.* (2010) Enhancement of RAD51 recombinase activity by the tumor suppressor PALB2. *Nat. Struct. Mol. Biol.* 17, 1255–1259
159. Buisson, R. *et al.* (2010) Cooperation of breast cancer proteins PALB2 and piccolo BRCA2 in stimulating homologous recombination. *Nat. Struct. Mol. Biol.* 17, 1247–1254
160. Deveryshetty, J. *et al.* (2019) Novel RNA and DNA strand exchange activity of the PALB2 DNA binding domain and its critical role for DNA repair in cells. *eLife* 8, e44063
161. Zhao, W. and Sung, P. (2015) Significance of ligand interactions involving Hop2-Mnd1 and the RAD51 and DMC1 recombinases in homologous DNA repair and XX ovarian dysgenesis. *Nucleic Acids Res.* 43, 4055–4066
162. Bizard, A.H. and Hickson, I.D. (2014) The dissolution of double Holliday junctions. *Cold Spring Harb. Perspect. Biol.* 6, a016477
163. Kramara, J. *et al.* (2018) Break-induced replication: The where, the why, and the how. *Trends Genet.* 34, 518–531
164. Barber, L.J. *et al.* (2008) RTEL1 maintains genomic stability by suppressing homologous recombination. *Cell* 135, 261–271
165. Xue, X. *et al.* (2015) Functions and regulation of the multitasking FANCM family of DNA motor proteins. *Genes Dev.* 29, 1777–1788
166. Aylon, Y. *et al.* (2004) The CDK regulates repair of double-strand breaks by homologous recombination during the cell cycle. *EMBO J.* 23, 4868–4875
167. Ira, G. *et al.* (2004) DNA end resection, homologous recombination and DNA damage checkpoint activation require CDK1. *Nature* 431, 1011–1017
168. Lin, S. *et al.* (2014) Enhanced homology-directed human genome engineering by controlled timing of CRISPR/Cas9 delivery. *eLife* 3, e04766
169. Gutschner, T. *et al.* (2016) Post-translational regulation of Cas9 during G1 enhances homology-directed repair. *Cell Rep.* 14, 1555–1566
170. Brinkman, E.K. *et al.* (2018) Kinetics and fidelity of the repair of Cas9-induced double-strand DNA breaks. *Mol. Cell* 70, 801–813
171. Shi, X. *et al.* (2019) Cas9 has no exonuclease activity resulting in staggered cleavage with overhangs and predictable di- and tri-nucleotide CRISPR insertions without template donor. *Cell Discov.* 5, 53
172. Isaac, R.S. *et al.* (2016) Nucleosome breathing and remodeling constrain CRISPR-Cas9 function. *eLife* 5, e13450
173. Schep, R. *et al.* (2020) Impact of chromatin context on Cas9-induced DNA double-strand break repair pathway balance. *bioRxiv* Published online May 5, 2020. https://doi.org/10.1101/2020.05.05.078436
174. Clouaire, T. and Legube, G. (2019) A snapshot on the Cis chromatin response to DNA double-strand breaks. *Trends Genet.* 35, 330–345
175. Canaj, H. *et al.* (2019) Deep profiling reveals substantial heterogeneity of integration outcomes in CRISPR knock-in experiments. *bioRxiv* Published online November 13, 2019. https://doi.org/10.1101/841098
176. Alexiadis, V. and Kadonaga, J.T. (2002) Strand pairing by Rad54 and Rad51 is enhanced by chromatin. *Genes Dev.* 16, 2767–2771
177. Cruz-Becerra, G. and Kadonaga, J.T. (2020) Enhancement of homology-directed repair with chromatin donor templates in cells. *eLife* 9, e55780
178. Hisano, Y. *et al.* (2015) Precise in-frame integration of exogenous DNA mediated by CRISPR/Cas9 system in zebrafish. *Sci. Rep.* 5, 8841
179. Zhang, J.P. *et al.* (2017) Efficient precise knockin with a double cut HDR donor after CRISPR/Cas9-mediated double-stranded DNA cleavage. *Genome Biol.* 18, 35
180. Yoshimi, K. *et al.* (2016) ssODN-mediated knock-in with CRISPR-Cas for large genomic regions in zygotes. *Nat. Commun.* 7, 10431
181. Shao, Y. *et al.* (2014) CRISPR/Cas-mediated genome editing in the rat via direct injection of one-cell embryos. *Nat. Protoc.* 9, 2493–2512
182. Paulsen, B.S. *et al.* (2017) Ectopic expression of RAD52 and dn53BP1 improves homology-directed repair during CRISPR-Cas9 genome editing. *Nat. Biomed. Eng.* 1, 878–888
183. Hanscom, T. and McVey, M. (2020) Regulation of error-prone DNA double-strand break repair and its impact on genome evolution. *Cells* 9, 1657
184. Stinson, B.M. *et al.* (2020) A mechanism to minimize errors during non-homologous end joining. *Mol. Cell* 77, 1080–1091.e8
185. Kosicki, M. *et al.* (2018) Repair of double-strand breaks induced by CRISPR-Cas9 leads to large deletions and complex rearrangements. *Nat. Biotechnol.* 36, 765–771
186. Adikusuma, F. *et al.* (2018) Large deletions induced by Cas9 cleavage. *Nature* 560, E8–E9
187. Korablev, A. *et al.* (2020) On-target CRISPR/Cas9 activity can cause undesigned large deletion in mouse zygotes. *Int. J. Mol. Sci.* 21, 3604
188. Cullot, G. *et al.* (2019) CRISPR-Cas9 genome editing induces megabase-scale chromosomal truncations. *Nat. Commun.* 10, 1136
189. Ishino, Y. *et al.* (1987) Nucleotide sequence of the *iap* gene, responsible for alkaline phosphatase isozyme conversion in *Escherichia coli*, and identification of the gene product. *J. Bacteriol.* 169, 5429–5433
190. Mojica, F.J. *et al.* (1993) Transcription at different salinities of *Haloferax mediterranei* sequences adjacent to partially modified PstI sites. *Mol. Microbiol.* 9, 613–621
191. Mojica, F.J. *et al.* (1995) Long stretches of short tandem repeats are present in the largest replicons of the Archaea Haloferax mediterranei and *Haloferax volcanii* and could be involved in replicon partitioning. *Mol. Microbiol.* 17, 85–93
192. Barrangou, R. *et al.* (2007) CRISPR provides acquired resistance against viruses in prokaryotes. *Science* 315, 1709–1712
193. Brouns, S.J. *et al.* (2008) Small CRISPR RNAs guide antiviral defense in prokaryotes. *Science* 321, 960–964
194. Marraffini, L.A. and Sontheimer, E.J. (2008) CRISPR interference limits horizontal gene transfer in staphylococci by targeting DNA. *Science* 322, 1843–1845
195. Garneau, J.E. *et al.* (2010) The CRISPR/Cas bacterial immune system cleaves bacteriophage and plasmid DNA. *Nature* 468, 67–71
196. Hale, C.R. *et al.* (2009) RNA-guided RNA cleavage by a CRISPR RNA-Cas protein complex. *Cell* 139, 945–956
197. Makarova, K.S. *et al.* (2020) Evolutionary classification of CRISPR-Cas systems: a burst of class 2 and derived variants. *Nat. Rev. Microbiol.* 18, 67–83
198. Deltcheva, E. *et al.* (2011) CRISPR RNA maturation by trans-encoded small RNA and host factor RNase III. *Nature* 471, 602–607
199. Wright, A.V. *et al.* (2016) Biology and applications of CRISPR systems: Harnessing nature's toolbox for genome engineering. *Cell* 164, 29–44
200. Tsai, S.Q. and Joung, J.K. (2016) Defining and improving the genome-wide specificities of CRISPR-Cas9 nucleases. *Nat. Rev. Genet.* 17, 300–312